

Cytosolic abscisic acid activates guard cell anion channels without preceding Ca^{2+} signals

Victor Levchenko, Kai R. Konrad, Petra Dietrich, M. Rob G. Roelfsema, and Rainer Hedrich*

Department of Molecular Plant Physiology and Biophysics, Julius-von-Sachs Institute for Biosciences, Biocenter, Würzburg University, Julius-von-Sachs-Platz 2, D97082 Würzburg, Germany

Communicated by Winslow R. Briggs, Carnegie Institution of Washington, Stanford, CA, January 9, 2005 (received for review January 28, 2004)

The phytohormone abscisic acid (ABA) reports on the water status of the plant and induces stomatal closure. Guard cell anion channels play a central role in this response, because they mediate anion efflux, and in turn, cause a depolarization-induced K^+ release. We recorded early steps in ABA signaling, introducing multibarreled microelectrodes in guard cells of intact plants. Upon external ABA treatment, anion channels transiently activated after a lag phase of ≈ 2 min. As expected for a cytosolic ABA receptor, iontophoretic ABA loading into the cytoplasm initiated a rise in anion current without delay. These ABA responses could be elicited repetitively at resting and at largely depolarized potentials (e.g., 0 mV), ruling out signal transduction by means of hyperpolarization-activated calcium channels. Likewise, ABA stimulation did not induce a rise in the cytosolic free-calcium concentration. However, the presence of ≈ 100 nM background Ca^{2+} was required for anion channel function, because the action of ABA on anion channels was repressed after loading of the Ca^{2+} chelator 1,2-bis(2-aminophenoxy)ethane-*N,N,N',N'*-tetraacetate. The chain of events appears very direct, because none of the tested putative ABA-signaling intermediates (inositol 1,4,5 trisphosphate, inositol hexakisphosphate, nicotinic acid adenine dinucleotide phosphate, and cyclic ADP-ribose), could mimic ABA as anion channel activator. In patch-clamp experiments, cytosolic ABA also evoked anion current transients carried by R- and S-type anion channels. The response was dose-dependent with half-maximum activation at 2.6 μM ABA. Our studies point to an ABA pathway initiated by ABA binding to a cytosolic receptor that within seconds activates anion channels, and in turn, leads to depolarization of the plasma membrane.

stomatal closure

The plant hormone abscisic acid (ABA) provides a developmental signal serving as a chemical switch between, for instance, dormancy and growth of seeds and buds (1). Furthermore, this sesquiterpene is involved in the transmission of environmental changes like drought, saline, and cold periods into stress-adaptation processes (2). Based on the time scale of the individual ABA responses, they can be subdivided into fast (seconds up to minutes) and slow (hours up to days, or even months) signaling processes. Stomatal closure represents the fastest ABA response known so far, characterized by a half-time of ≈ 5 min, and presumably does not involve gene activation. Fast stomatal closure is accomplished by the release of potassium and chloride via voltage-dependent ion channels and by metabolic degradation of the major organic anion malate (3, 4).

In search for ABA signaling intermediates, guard cells have been challenged with well characterized modulators operating in signal transduction pathways of animal cells (5–8). To a large extent, the respective substances were injected into guard cells of excised epidermal peels, and the corresponding responses were monitored (9–12). After microinjection, photolysis of caged inositol 1,4,5 trisphosphate (InsP_3) was shown to initiate a rise in cytoplasmic Ca^{2+} , indicating a release of Ca^{2+} from internal stores (10). With a similar approach, injection of cyclic ADP (cADP)-ribose was shown to induce sustained or oscillatory Ca^{2+} rises (12), suggesting a role for both compounds as

intermediates of the ABA-induced stomatal response. Furthermore, lipid-based signals (8), reactive oxygen species (5), nitric oxide (NO) (13) and G proteins (14) affect ion fluxes across the plasma and vacuolar membrane in guard cells, and thus were proposed to play a role in ABA-induced stomatal closure.

In addition, genes involved in ABA signaling were derived from mutants altered in ABA responsiveness (1, 5, 14, 15). The second messengers and genes identified have been incorporated into complex models that try to bridge the gap between the still unknown ABA receptor and stomatal closure (5, 14, 16). These models often are based on observations of short- and long-time ABA-responses, obtained with different guard cell preparations, various other cell types, and different species. Despite a large variation between existing models, all predict rises in cytoplasmic Ca^{2+} as a prerequisite for the activation of anion channels. This hypothesis is based on the Ca^{2+} -dependent activity of both R- (17) and S-type (18) anion channels found in the plasma membrane. Nevertheless, a direct link between the ABA-induced Ca^{2+} signal and the activation of anion channels has not yet been proven.

Materials and Methods

Patch Clamp. *Vicia faba* L. plants (Französische Weisskeimige, Gebag, Hannover, Germany) were grown in a greenhouse. Guard cell protoplasts were isolated according to methods described in ref. 17 and studied with the patch-clamp technique (17, 19) by using Kimax-51 glass (Kimble Products, Vineland, NY) coated with silicone (Sylgard 184 silicone elastomer kit, Dow-Corning). Currents were sampled with an EPC-7 patch-clamp amplifier (HEKA, Lambrecht, Germany) at 5 kHz and low-pass-filtered at 1 or 2 kHz for excised patch and whole-cell measurements, respectively. Liquid junction potentials were corrected offline (20). Protoplasts were characterized by a mean membrane capacitance of 4.9 ± 0.4 pF ($n = 133$). The pipette solution contained 150 mM tetraethylammonium chloride, 2 mM MgCl_2 , 10 mM EGTA, 1 mM MgATP, and 10 mM Hepes-Tris (pH 7.2), and the bath solution contained 40 mM CaCl_2 , 10 mM Mes-Tris (pH 5.6), and, if not otherwise mentioned, 100 μM LaCl_3 .

Recordings on Guard Cells Within Intact Leaves. Guard cells in intact plants were recorded as described (21), but, instead of double barreled-microelectrodes, triple-barreled microelectrodes were used. Two barrels were filled with 300 mM KCl or 300 mM CsCl to measure and clamp the membrane potential, and the third barrel was used for current injection and filled with 2 mM FURA-2, 0.1 mM ABA, 50 mM 1,2-bis(2-aminophenoxy)ethane-*N,N,N',N'*-tetraacetate (BAPTA) or putative second messengers InsP_3 , inositol hexakisphosphate, cADP-ribose, and nicotinic acid adenine dinucleotide phosphate at a concentration of 5 mM. All three barrels of the intracellular electrode

Abbreviations: ABA, abscisic acid; BAPTA, 1,2-bis(2-aminophenoxy)ethane-*N,N,N',N'*-tetraacetate; InsP_3 , inositol 1,4,5 trisphosphate; cADP-ribose, cyclic ADP-ribose.

*To whom correspondence should be addressed. E-mail: hedrich@botanik.uni-wuerzburg.de.

© 2005 by The National Academy of Sciences of the USA

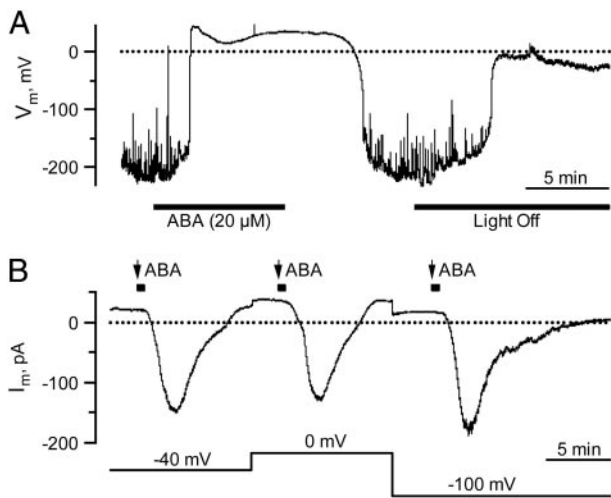


Fig. 1. Plasma membrane responses of *V. faba* guard cells in intact plants to ABA and light. (A) Reversible changes in the free-running membrane potential of a guard cell exposed to ABA and darkness. Note that K^+ conductances in A and B were eliminated with Ba^{2+} in the external solution and Cs^+ in the pipette. (B) Dependence of ABA-induced anion channel activation on the plasma membrane potential. ABA ($20 \mu M$) was applied with repetitive pulses of 40 s (black squares above the trace) to a single guard cell at three holding potentials (lower trace).

were connected to microelectrode amplifiers (VF-102, Bio-Logic, Claix, France). The membrane potential was clamped by using a differential amplifier (CA-100, Bio-Logic). Data were filtered at 250 Hz and sampled at 1 kHz during short pulses, or filtered at 12 Hz and sampled at 50 Hz for long-term registrations. The solution on the leaf surface contained 5 mM KCl, 5 mM K citrate (pH 5.0), 0.1 mM $CaCl_2$, and 0.1 mM $MgCl_2$. In Fig. 1, 5 mM $BaCl_2$ was used instead of 5 mM KCl.

Fluorescent Dye Loading and Microinjections. FURA-2 loading into the guard cell cytoplasm was achieved by iontophoretic microinjection from the third microelectrode barrel. The dye was loaded through current injection (up to -500 pA), whereas cells were kept at a holding potential of -100 mV. FURA concentrations were estimated, comparing the fluorescence intensity of guard cells in intact plants, with that of FURA-2 equilibrated protoplasts in the whole-cell patch-clamp configuration. Loading was stopped before the FURA-2 concentration exceeded $100 \mu M$. Cells in which the FURA-2 concentration dropped to $<13 \mu M$ during the experiment were eliminated from the analysis.

Movement of FURA-2 in guard cells was determined by scanning three regions of $28 \mu m^2$ within a single cell. One region was located at the place of injection, whereas the others were at the distant ends. The delay of a FURA-dependent rise in fluorescence at the distant ends was taken as a measure for movement of the dye. The flow of fluorescent dye was further studied with a confocal scanning module (QLC100, Visitron Systems, Puchheim, Germany). The third barrel was filled with 2 mM K-fluorescein, which was injected into the cytoplasm with a current of -500 pA. Confocal images were taken in a single plane every 2.2 s.

Ratiometric Fluorescence Spectroscopy. The dual-excitation wavelength of the Ca^{2+} -dependent fluorescent dye FURA-2 (Molecular Probes) was used to monitor the cytoplasmic free Ca^{2+} concentration. Ratiometric fluorescence spectroscopy measurements were carried out by using METAFLUOR software (Universal Imaging, Downingtown, PA). FURA-2 was excited with 200-ms flashes of UV light at 345 and 390 nm with a time interval

of 1 s (Visitron Systems). The emission signal was filtered with a 510-nm bandpass filter (D510/40 M, AF Analysentechnik, Tübingen, Germany) and captured with a cooled charge-coupled device camera (CoolSNAP HQ, Roper Scientific, Tucson, AZ). Background fluorescence levels of both wavelengths were taken from a reference region placed within a part of the unloaded neighboring guard cell. The intracellular free Ca^{2+} concentration was calculated according to ref. 22 by using the following equation:

$$[Ca^{2+}]_{free} = K_d \frac{(R - R_{min})F_{min}}{(R_{max} - R)F_{max}} \quad [1]$$

where, K_d represents the binding constant of FURA-2 for Ca^{2+} , R represents the 345/390 nm excitation ratio, and R_{min} and R_{max} correspond to Ca^{2+} -free and Ca^{2+} -saturated FURA-2, respectively. F_{min} and F_{max} give the fluorescence intensity measured at 390 nm with Ca^{2+} -free and Ca^{2+} -saturated FURA-2, respectively. We determined a K_d of 270 nM *in vitro* by using a Ca^{2+} calibration buffer kit with Mg^{2+} (Molecular Probes). R_{min} and F_{min} were defined as the values obtained after simultaneously injecting FURA-2 and BAPTA into the guard cell of intact plants. Subsequently, the values for R_{max} and F_{max} were obtained by clamping the plasma membrane to -500 mV, inducing a massive and saturating influx of Ca^{2+} .

Results

In previous studies (21, 23, 24), we used multibarreled microelectrodes impaled into guard cells of intact plants to record plasma membrane responses to blue and red light, CO_2 , and ABA. Here, we extended this method by injecting the Ca^{2+} reporter dye FURA-2 to simultaneously monitor ABA-induced changes in the cytoplasmic free Ca^{2+} concentration and anion channel activity. This combination of methods should establish the role of Ca^{2+} signals or Ca^{2+} oscillations in ABA-induced stomatal closure (9, 25–31), or provide evidence for Ca^{2+} -independent pathways (9, 26, 32, 33).

ABA Activates Anion Channels Without Rise in Cytosolic Ca^{2+} . Guard cells in intact plants previously were found to hyperpolarize in the light, to an average membrane potential of -110 mV (21). To enable recordings of anion channel conductance at depolarized potentials, K^+ channels can be blocked by extracellular Ba^{2+} and intracellular Cs^+ (24). Under these conditions (21), the average guard cell membrane potential was further hyperpolarized and fluctuated, probably due to small changes in channel activities (Fig. 1A). Upon addition of $20 \mu M$ external ABA, the membrane depolarized within 2 min to ≈ 40 mV (Fig. 1A), the predicted Nernst potential for chloride. This finding indicates that ABA activates anion channels. After the removal of the stress hormone, the membrane repolarized again. When the light was switched off, the cells depolarized too, although to less extreme values (Fig. 1A). Thus, under the given experimental conditions, guard cells are ABA- and light-sensitive.

In the voltage-clamp mode, external application of ABA triggered anion current transients after a lag phase (time required to get 10% of the maximum response) of 2.2 min (SD = 1.0, $n = 13$) (Figs. 1B and 2A). Similar ABA-induced anion efflux transients could be observed in intact *Nicotiana tabacum* and *Commelina communis* plants, too (data not shown). To test whether ABA activates anion channels via opening of hyperpolarization-activated calcium channels, we recorded ABA-induced changes in plasma membrane ion currents at different holding potentials. In response to 40-s pulses of external ABA, anion current transients were recorded at -40 , 0, and -100 mV (Fig. 1B). At all holding potentials, the delay after stimulus onset, and amplitude and kinetics of the ABA responses were comparable, indicating that the ABA response did not depend on the

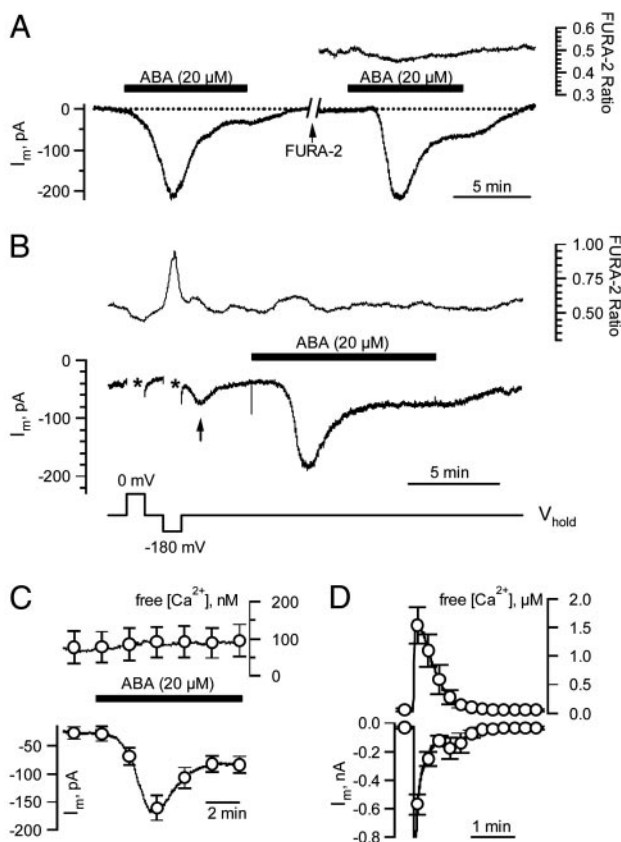


Fig. 2. Simultaneous recordings of the cytoplasmic free $[Ca^{2+}]$ and ABA-induced anion currents. (A) ABA responses of a *V. faba* guard cell in an intact plant, recorded at a holding potential of -100 mV before and after injection of FURA-2. (Left) Response to ABA before loading. (Right) ABA response after loading of FURA-2. The upper trace shows the FURA-2 F_{345}/F_{390} fluorescent ratio. (B) Guard cell stimulated with voltage pulses and ABA. A FURA-2 loaded guard cell was clamped to a holding potential of -100 mV and to test potentials of 0 and -180 mV (lower trace). Hyperpolarization, but not depolarization, evoked an increase in cytoplasmic free $[Ca^{2+}]$ (upper trace), followed by an increase in inward current (arrow, middle trace). Subsequent application of ABA (black bar) induced an inward current without a change in cytoplasmic free $[Ca^{2+}]$. (C) Average change in cytoplasmic free $[Ca^{2+}]$ (upper trace) of six guard cells displaying typical ABA-induced anion currents (lower trace). Note that ABA did not affect the cytoplasmic free $[Ca^{2+}]$. Error bars represent SE. (D) Average change in cytoplasmic free $[Ca^{2+}]$ (upper trace) of 11 guard cells clamped to -275 mV for 1 s, starting after 20 s, from a holding potential of -100 mV. Note that strong hyperpolarizations triggered large changes in the cytoplasmic free $[Ca^{2+}]$ and were followed by a transient increase in inward current. Error bars represent SE.

holding potential. The induction of inward current transients at largely depolarized potentials indicates that hyperpolarization-activated calcium channels (5) are not involved in the ABA-dependent activation of anion channels.

To link the ABA-induced activation of anion channels to cytoplasmic Ca^{2+} signals, we iontophoretically injected the calcium reporter dye FURA-2 by means of the third barrel of the microelectrode system. FURA-2 loading into the guard cell cytoplasm to concentrations up to $100 \mu M$ did not interfere with the ABA response because similar anion current transients were recorded before and after the dye injection (Fig. 2A). Despite the pronounced response of anion channels to ABA, no changes in the cytosolic Ca^{2+} concentration were recorded (Fig. 2A, upper trace). Because, in isolated protoplasts, anion channels are activated by Ca^{2+} (17, 18), we tested whether this activation mode functions in guard cells of intact plants, too. For this

purpose, we manipulated the cytoplasmic free Ca^{2+} concentrations by means of changes in the membrane potential (Fig. 2B). Upon depolarization, the cytoplasmic Ca^{2+} level dropped slightly (the first asterisk in Fig. 2B), whereas a hyperpolarizing voltage pulse induced an increase in the cytoplasmic Ca^{2+} concentration (the second asterisk in Fig. 2B). Apparently, hyperpolarization-activated Ca^{2+} channels are operating in these cells (34, 35). In line with the Ca^{2+} dependence of anion channels (17, 18), the Ca^{2+} elevation triggered at -180 mV was followed by a transient inward current (arrow in Fig. 2B). In contrast to hyperpolarization, external application of ABA did not induce an increase in cytosolic Ca^{2+} , but nevertheless elicited a large anion current (Fig. 2B). In six cells displaying a large ABA-induced anion channel activity, the cytoplasmic free Ca^{2+} concentration remained at a basic level of ≈ 100 nM (Fig. 2C). In contrast, we found that strong hyperpolarizing pulses to -275 mV evoked large rises in cytoplasmic Ca^{2+} (Fig. 2D). The hyperpolarization-induced Ca^{2+} rises were followed by large inward currents lasting for ≈ 2 min (Fig. 2D), and thus decayed much faster (transients were shorter) than those triggered by ABA (Figs. 1B and 2A and B). This finding confirms that a rise in the cytoplasmic free Ca^{2+} concentration can activate anion channels (17, 18), but cytoplasmic calcium signals are not required for the ABA-induced activation of anion channels in guard cells of intact plants.

To lower the resting cytoplasmic free Ca^{2+} level, we loaded the calcium chelator BAPTA simultaneously with FURA-2. The cytoplasmic BAPTA concentration was estimated to range from 0.65 to 1.5 mM, assuming equal loading properties of BAPTA and FURA-2. Under control conditions, ABA evoked normal anion current transients; however, this ABA response was repressed after loading of BAPTA (Fig. 3A). This finding indicates that a background level of cytoplasmic Ca^{2+} is required for the ABA-induced anion channel activation.

ABA Activates Anion Channels by Means of a Cytosolic Receptor. ABA perception has been suggested to occur either at the external (36) or cytoplasmic side of the plasma membrane (9, 37). To distinguish between the two sites, we loaded ABA iontophoretically into guard cells of intact plants. Current injection with the triple-barreled microelectrode system was carried out in the voltage-clamp mode, keeping the plasma membrane stable at -100 mV. The inward current applied during dye or ABA injection was thus automatically compensated by an outward current of the same magnitude. By using confocal imaging, we could demonstrate that cytosolic streaming is maintained during this loading procedure (Movies 1 and 2, which are published as supporting information on the PNAS web site). Iontophoretically loaded molecules like FURA-2 are therefore distributed throughout the cell within 33 s (SD 11 , $n = 8$). After an anion current transient induced by external ABA application, we loaded ABA into the cytoplasm of guard cells in intact leaves (arrows in Fig. 3B). In the latter case, anion current transients were elicited too, but, in contrast to external application, anion currents now activated without a significant lag phase. The activation of anion channels was not due to current application, since the injection of FURA2 (not shown) or nonpotent substances (Fig. 3C) was not followed by increases in inward current. As with external application (Fig. 1B), repetitive pulses of cytoplasmic ABA triggered consecutive anion current transients (Fig. 3B). In a similar experiment, up to seven transients could be elicited in a single cell without pronounced desensitization (data not shown). Together, the data presented so far point to an ABA receptor located in the cytosol or on the cytosolic side of the plasma membrane. The delay observed with external ABA stimulation thus seems to reflect the time required for the hormone to cross the cell wall and plasma membrane.

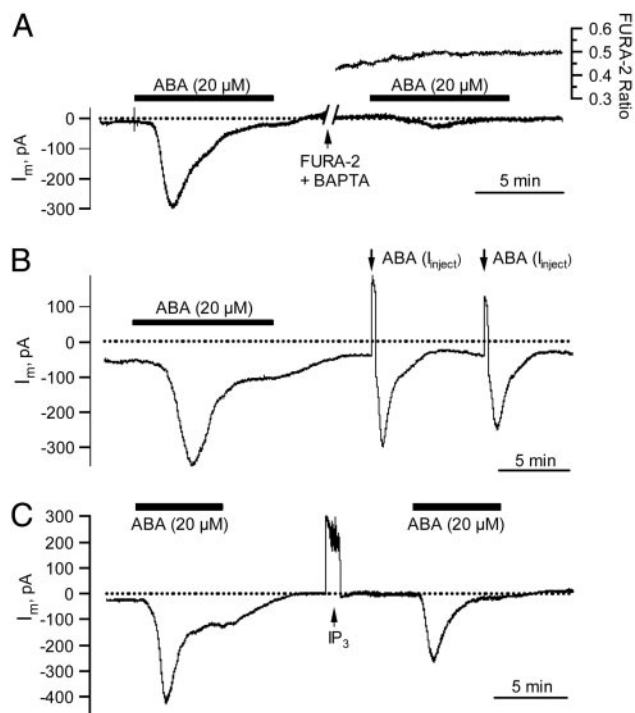


Fig. 3. Cytoplasmic application of BAPTA, ABA, and the putative second messenger $InsP_3$. (A) Repression of the ABA-induced anion current transient by cytoplasmic BAPTA. (Left) Response to external ABA before loading BAPTA. (Right) Strong inhibition of the ABA response after simultaneous loading of BAPTA and FURA-2. The cell was loaded by means of the third barrel of the microelectrode filled with 2 mM FURA-2 and 50 mM BAPTA. Upper trace shows the FURA-2 F_{345}/F_{390} fluorescent ratio. (B) Guard cell response to externally and cytoplasmically applied ABA. Anion current transients were triggered with ABA externally (black bar) and subsequently through a 30-s loading pulse of ABA by means of the third barrel of the microelectrode filled with 100 μ M ABA (arrows). Note that during injection the membrane potential remained clamped at -100 mV, the inward loading current by means of the third barrel, therefore, is compensated by an outward current. (C) Current response to the putative signaling intermediate $InsP_3$. Before and after $InsP_3$ injection, anion current transients were elicited with extracellular ABA (black bars) at a holding potential of -100 mV.

Putative ABA-Signaling Intermediates Do Not Mimic ABA Action. In search for ABA-signaling intermediates able to replace the stress hormone with respect to channel activation, we used a protocol similar to that in Fig. 3B. After an ABA-induced current transient, potential signaling intermediates were loaded iontophoretically into the cytosol of guard cells. The ABA responsiveness of the cell was reexamined with a second ABA pulse (Fig. 3C, exemplified for $InsP_3$). This protocol guaranteed that putative signaling intermediates were only tested in ABA-responsive cells. Among the tested substances, $InsP_3$ (Fig. 3C), inositol hexakisphosphate, and nicotinic acid adenine dinucleotide phosphate (38) did not evoke anion current transients ($n = 6$ for each compound). Application of cADP-ribose, however, elicited transient inward currents in 8 of 18 cells (Fig. 6A, which is published as supporting information on the PNAS web site). In four other cells, the inward current steadily increased until the cell was dominated by large S-type currents and collapsed (Fig. 6B).

Cytosolic ABA Activates R- and S-Type Anion Channels in Isolated Protoplasts. Previous studies (24, 39) have shown that the ABA-evoked anion currents are carried by rapidly activating and inactivating (R-type), and slowly activating, noninactivating (S-type) anion channels (24, 39, 40). However, in isolated guard cell

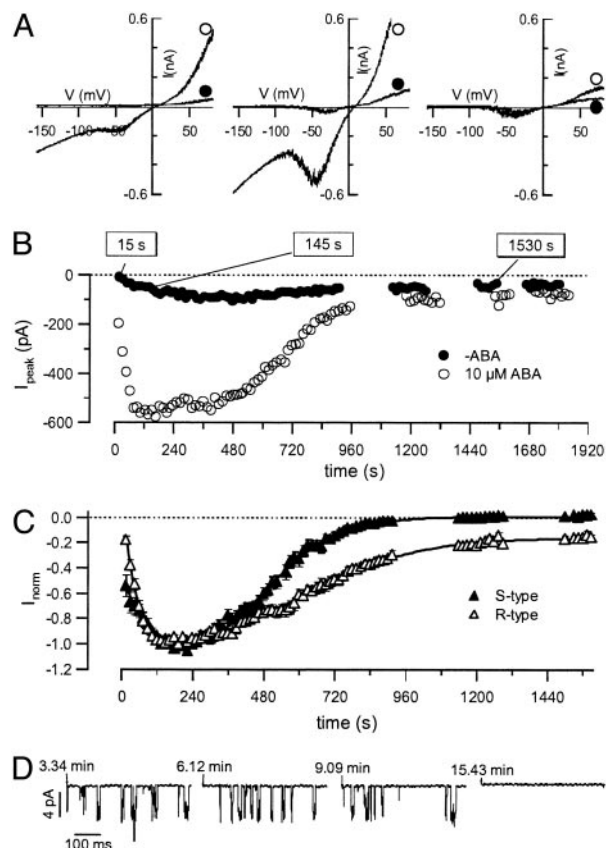


Fig. 4. Kinetics of ABA-induced activation of anion channels in guard cell protoplasts. (A) Current-voltage relations in the presence of 10 μ M cytosolic ABA, (open symbols) and without ABA (filled symbols), at time points indicated. Voltage ramps were applied from -158 to $+82$ mV in 1,500 ms, and the holding potential was -158 mV. Note the activities of R- and S-type channels. (B) Time courses of peak currents from voltage ramps as shown in Upper, recorded after whole-cell access. Time courses are shown for representative experiments in the absence (filled symbols, $n = 26$) and presence (open symbols, $n = 24$) of 10 μ M ABA in the pipette solution. (C) Peak currents of R- and S-type channels were plotted as a function of time after gaining whole-cell access. Currents were normalized to their maxima. S-type current amplitudes were determined from linear interpolation between the current at -98 and 2 mV during voltage ramps as shown in A. R-type current amplitudes were expressed as the difference between peak and S-type currents. (D) Single-channel fluctuations of an outside-out patch, excised from a whole cell at the peak of ABA-induced anion currents (≈ 2 min). The recordings were conducted at several time points, indicated as the time after gaining whole-cell access.

protoplasts, long-term incubation with ABA induced activation of S-type channels only (40). To study the contribution of R- and S-type channels to overall anion currents elicited by cytoplasmic ABA, we performed patch-clamp experiments. ABA, applied by means of the patch pipette, triggered anion current transients carried by R- and S-type channels (Fig. 4A). The ABA-induced activation of both channels types is in line with the recordings on guard cells in intact plants (24) but has not been recognized for guard cell protoplasts before. After whole-cell access in the presence of 10 μ M cytosolic ABA, anion currents reached a peak after ≈ 2 min and slowly returned to background levels again (Fig. 4B). This response was observed with 100 μ M La^{3+} in the bath solution to block hyperpolarization activated Ca^{2+} channels (34, 35) (Figs. 4 and 5) and without La^{3+} (data not shown). In the absence of ABA, only small anion channel activities were apparent. Whereas the activation time course was similar for both channel types, the deactivation was faster and more complete for S-type channels compared with R-type channels (Fig.

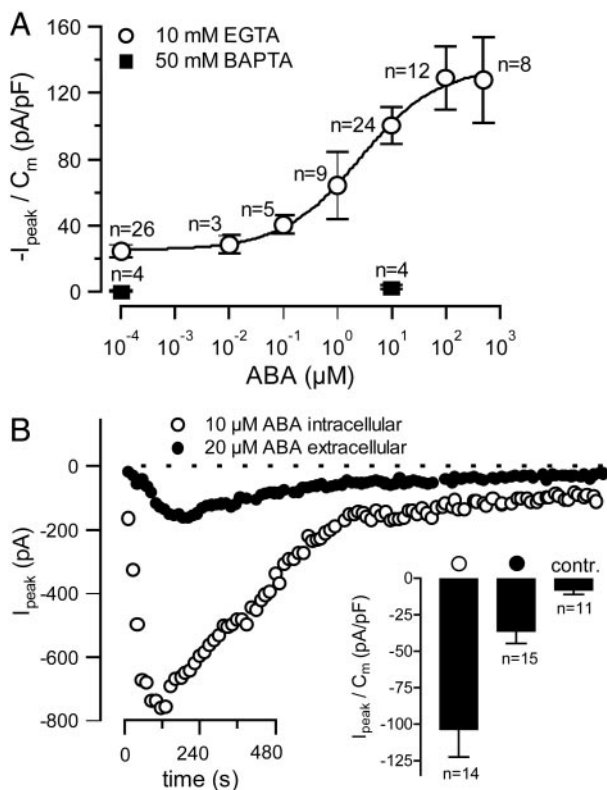


Fig. 5. Activation of anion currents in guard cell protoplasts by extracellular and intracellular ABA. (A) Voltage ramps in the presence of different ABA concentrations in the pipette solution were applied and peak currents were determined, as in Fig. 4. The maximum currents during the ABA responses were normalized to the cell capacitance and plotted as a function of the ABA concentration (error bars represent SE, n indicates number of cells). Two cells with unusually high ABA responses were not included in the analysis. Filled symbols represent data obtained with a pipette solution containing 50 mM BAPTA instead of 10 mM EGTA. (B) Time courses of peak currents from voltage ramps as shown in Fig. 4A Upper, recorded after whole-cell access. Time courses are shown for representative experiments in which 20 μ M ABA was given at the extracellular face (filled symbols) or 10 μ M ABA was applied by means of the pipette solution (open symbols). (Inset) Average peak currents after intracellular (open symbols), or extracellular (filled symbols) ABA application, or without ABA (contr.). Error bars represent SE, n indicates number of cells.

4C). When, after ABA-activation of R-type channels in the whole-cell configuration, an outside-out patch was excised, the activity of single 68-pS channels could be monitored (Fig. 4D). The same conductance also has been determined in the absence of ABA (41), and indicates an increased open probability of the channel, rather than a change in single-channel conductance.

In the patch-clamp experiments shown in Fig. 4, the pipette solutions contained 10 μ M ABA together with 10 mM EGTA. Under these conditions, the cytosolic Ca^{2+} level appeared to be sufficiently high to maintain anion channels in the active state (Fig. 4A and B). In contrast, the presence of 50 mM BAPTA in the pipette solution prevented anion channel activation (filled symbols in Fig. 5A), just as BAPTA repressed ABA-induced activation of anion channels in guard cells of intact plants (Fig. 3A).

To obtain a dose-response relation for ABA-dependent anion currents, we varied the ABA concentration in the pipette solution. Anion current densities occurring at the peak of the ABA-induced transient (see Fig. 4B) were plotted against the hormone concentration, revealing a half-maximal concentration of 2.6 μ M (\pm)-cis, trans-ABA (Fig. 5A). Both R- and S-type

anion channels were also activated by external ABA, but this response was slower and less pronounced compared with intracellular ABA application (Fig. 5B). Internal ABA (10 μ M) elicited anion currents that peaked after 2.8 min (SE = 0.4, n = 14), whereas 20 μ M ABA applied at the extracellular face caused a peak current after 4.0 min only (SE = 0.3, n = 15). Apparently, ABA activates anion channels more efficiently from the cytosolic side as compared with the extracellular side. This result, together with the rapid response to iontophoretically loaded ABA of guard cell in intact plants, points to an intracellular ABA receptor.

Discussion

ABA regulates a set of ion transporters in guard cells that are associated with fast stomatal closure. In addition, this stress hormone has a large impact on gene activation in several cell types. The gene transcription induced by ABA, however, differs between different cell types (16, 42). ABA-signaling pathways, targets, or models, therefore, should not be generalized for all cell types of the plant. Here, we focused on the activation of anion channels essential for the ABA-induced depolarization that initiates ion efflux from guard cells, and finally leads to stomatal closure. In addition, deactivation of H^{+} -ATPases may contribute to the depolarization, as was recently shown for suspension cells of *Arabidopsis thaliana* (43). Although ABA inhibition of H^{+} -ATPases was also reported for guard cells (44), the changes in H^{+} current (45) will be masked by the massive increase in anion channel activity recorded for guard cells in intact plants. The fast hyperpolarization of guard cells after ABA removal (Fig. 1A) indicates that H^{+} -ATPases are reactivated rapidly, but the dynamics of this ABA response still await a more detailed examination.

A role for cytoplasmic Ca^{2+} has been suggested for a large number of ABA responses (1, 5). In guard cells, ABA was found to induce steady, transient, or repetitive rises in the cytoplasmic Ca^{2+} concentration (25, 26, 29, 46). However, in some cells, ABA could also turn spontaneous Ca^{2+} oscillations off (47). In guard cells of *A. thaliana*, ABA-induced Ca^{2+} oscillations occur with a period of 10.3 min (31), and are therefore too slow to encode a signal that activates anion channels with a lag time of 2 min, as observed in the present study for guard cells in intact plants. Furthermore, by using the Ca^{2+} indicator FURA-2 we could not observe a rise in cytoplasmic free Ca^{2+} preceding or accompanying the activation of anion channels. Apparently, the activation of anion channels by ABA occurs via a Ca^{2+} -independent switch for *V. faba* guard cells impaled in intact plants. In favor of a control mechanism independent of a Ca^{2+} influx by means of the plasma membrane, anion channels could be activated in the presence of 100 μ M La^{3+} (Fig. 4A). This inhibitor blocks hyperpolarization-activated Ca^{2+} channels at the concentration used (34, 35). Furthermore, in intact plants, ABA also activates anion channels at far depolarized plasma membrane potentials (Fig. 1B). These data provide strong evidence that hyperpolarization-activated Ca^{2+} channels are not involved in ABA-induced anion channel activation. Although we found that a rise in the cytoplasmic Ca^{2+} concentration was not necessary for anion channel activation, a basic Ca^{2+} level is required for this response. BAPTA-loaded intact guard cells and protoplasts exhibited virtually no ABA responses (Figs. 3A and 5A). In line with these results, *C. communis* guard cells injected with BAPTA do not close after ABA application (30).

Guard cell responses could be evoked by ABA applied externally, but they were faster and more pronounced when ABA was applied directly to the cytoplasm. This behavior points to an internal perception site for ABA, which initiates a Ca^{2+} -independent activation of anion channels. An internal perception site was also concluded from studies on stomatal closure after photolysis of caged ABA (9) and from patch-clamp studies

on the ABA inhibition of inward K^+ channels (37). Additional ABA receptors or ABA translocators may be located at the external site of the plasma membrane, as suggested by ABA-binding studies (48) and gene expression in suspension-cultured cells (42, 49–51).

We conclude that fast activation of R- and S-type anion channels by ABA is initiated in the cytoplasm and involves a robust and direct pathway that does not involve a rise in cytoplasmic free Ca^{2+} . The activation of this ABA pathway could not be triggered through the injection of $InsP_3$, inositol hexakisphosphate, nicotinic acid adenine dinucleotide phosphate, or cADP-ribose. This response may thus differ from long-term effects, such as Ca^{2+} -dependent gene activation, as

has been suggested for ABA-induced expression of GORK and RAB18 in *Arabidopsis* suspension-cultured cells (42, 50, 51). For short-term regulation of anion channel activity in guard cells, ABA-sensitive but Ca^{2+} -independent signaling components such as the protein kinases OST1/AAPK (15, 52), or the protein phosphatases ABI 1/2 (53, 54), represent good candidates. These ABA-signaling intermediates may modulate R- and S-type anion channels by means of a mechanism acting parallel to the well established Ca^{2+} dependence (17, 18), or they may alter the Ca^{2+} sensitivity of these anion channels.

We thank D. Guinot for assistance with the fluorescence calibration. This work was supported by Sonderforschungsbereich 567 and other grants of the Deutsche Forschungsgemeinschaft (to R.H.).

1. Finkelstein, R. R., Gampala, S. S. L. & Rock, C. D. (2002) *Plant Cell* **14**, S15–S45.
2. Chinnusamy, V., Schumaker, K. & Zhu, J. K. (2004) *J. Exp. Bot.* **55**, 225–236.
3. Raschke, K., Hedrich, R., Reckmann, U. & Schroeder, J. I. (1988) *Bot. Acta* **101**, 283–294.
4. MacRobbie, E. A. C. (1987) in *Stomatal Function*, eds. Zeiger, E., Farquhar, G. D. & Cowan I. R. (Stanford Univ. Press, Stanford CA), pp. 125–162.
5. Schroeder, J. I., Allen, G. J., Hugouvieux, V., Kwak, J. M. & Waren, D. (2001) *Ann. Rev. Plant Physiol. Plant Mol. Biol.* **52**, 627–658.
6. Sanders, D., Pelloux, J., Brownlee, C. & Harper, J. F. (2002) *Plant Cell* **14**, S401–S417.
7. Assmann, S. M. & Wang, X. Q. (2001) *Curr. Opin. Plant Biol.* **4**, 421–428.
8. Hetherington, A. M. (2001) *Cell* **107**, 711–714.
9. Allan, A. C., Fricker, M. D., Ward, J. L., Beale, M. H. & Trewavas, A. J. (1994) *Plant Cell* **6**, 1319–1328.
10. Gilroy, S., Read, N. D. & Trewavas, A. J. (1990) *Nature* **346**, 769–771.
11. Blatt, M. R., Thiel, G. & Trentham, D. R. (1990) *Nature* **346**, 766–769.
12. Leckie, C. P., McAinsh, M. R., Allen, G. J., Sanders, D. & Hetherington, A. M. (1998) *Proc. Natl. Acad. Sci. USA* **95**, 15837–15842.
13. Garcia-Mata, C., Gay, R., Sokolowski, S., Hills, A., Lamattina, L. & Blatt, M. R. (2003) *Proc. Natl. Acad. Sci. USA* **100**, 11116–11121.
14. Jones, A. M. & Assmann, S. M. (2004) *EMBO Rep.* **5**, 572–578.
15. Mustilli, A. C., Merlot, S., Vavasseur, A., Fenzi, F. & Giraudat, J. (2002) *Plant Cell* **14**, 3089–3099.
16. Leonhardt, N., Kwak, J. M., Robert, N., Waner, D., Leonhardt, G. & Schroeder, J. I. (2004) *Plant Cell* **16**, 596–615.
17. Hedrich, R., Busch, H. & Raschke, K. (1990) *EMBO J.* **9**, 3889–3892.
18. Schroeder, J. I. & Hagiwara, S. (1989) *Nature* **338**, 427–430.
19. Hamill, O. P., Marty, A., Neher, E., Sakmann, B. & Sigworth, F. J. (1981) *Eur. J. Phys.* **391**, 85–100.
20. Neher, E. (1992) *Methods Enzymol.* **207**, 123–131.
21. Roelfsema, M. R. G., Steinmeyer, R., Staal, M. & Hedrich, R. (2001) *Plant J.* **26**, 1–13.
22. Gryniewicz, G., Poenie, M. & Tsien, R. Y. (1985) *J. Biol. Chem.* **260**, 3440–3450.
23. Roelfsema, M. R. G., Hanstein, S., Felle, H. H. & Hedrich, R. (2002) *Plant J.* **32**, 65–75.
24. Roelfsema, M. R. G., Levchenko, V. & Hedrich, R. (2004) *Plant J.* **37**, 578–588.
25. McAinsh, M. R., Brownlee, C. & Hetherington, A. M. (1990) *Nature* **343**, 186–188.
26. Gilroy, S., Fricker, M. D., Read, N. D. & Trewavas, A. J. (1991) *Plant Cell* **3**, 333–344.
27. McAinsh, M. R., Webb, A. A. R., Staxen, I., Taylor, J. E. & Hetherington, A. M. (1995) *Plant Physiol.* **7**, 1207–1219.
28. Grabov, A. & Blatt, M. R. (1998) *Proc. Natl. Acad. Sci. USA* **95**, 4778–4783.
29. Staxen, I., Pical, C., Montgomery, L. T., Gray, J. E., Hetherington, A. M. & McAinsh, M. R. (1999) *Proc. Natl. Acad. Sci. USA* **96**, 1779–1784.
30. Webb, A. A., Larman, M. G., Montgomery, L. T., Taylor, J. E. & Hetherington, A. M. (2001) *Plant J.* **26**, 351–362.
31. Allen, G. J., Chu, S. P., Harrington, C. L., Schumacher, K., Hoffmann, T., Tang, Y. Y., Grill, E. & Schroeder, J. I. (2001) *Nature* **411**, 1053–1057.
32. Schwarz, M. & Schroeder, J. I. (1998) *FEBS Lett.* **428**, 177–182.
33. Romano, L. A., Jacob, T., Gilroy, S. & Assmann, S. M. (2000) *Planta* **211**, 209–217.
34. Pei, Z. M., Murata, Y., Benning, G., Thomine, S., Klusener, B., Allen, G. J., Grill, E. & Schroeder, J. I. (2000) *Nature* **406**, 731–734.
35. Hamilton, D. W., Hills, A., Kohler, B. & Blatt, M. R. (2000) *Proc. Natl. Acad. Sci. USA* **97**, 4967–4972.
36. Anderson, B. E., Ward, J. M. & Schroeder, J. I. (1994) *Plant Physiol.* **104**, 1177–1183.
37. Schwartz, A., Wu, W. H., Tucker, E. B. & Assmann, S. M. (1994) *Proc. Natl. Acad. Sci. USA* **91**, 4019–4023.
38. Navazio, L., Bewell, M. A., Siddiqua, A., Dickinson, G. D., Galione, A. & Sanders, D. (2000) *Proc. Natl. Acad. Sci. USA* **97**, 8693–8698.
39. Raschke, K., Shabahang, M. & Wolf, R. (2003) *Planta* **217**, 639–650.
40. Pei, Z. M., Kuchitsu, K., Ward, J. M., Schwarz, M. & Schroeder, J. I. (1997) *Plant Cell* **9**, 409–423.
41. Dietrich, P. & Hedrich, R. (1998) *Plant J.* **15**, 479–487.
42. Becker, D., Hoth, S., Ache, P., Wenkel, S., Roelfsema, M. R. G., Meyerhoff, O., Hartung, W. & Hedrich, R. (2003) *FEBS Lett.* **554**, 119–126.
43. Brault, M., Amiar, Z., Pennarun, A. M., Monestiez, M., Zhang, Z., Cornel, D., Dellis, O., Knight, H., Bouteau, F. & Rona, J. P. (2004) *Plant Physiol.* **135**, 231–243.
44. Goh, C. H., Kinoshita, T., Oku, T. & Shimazaki, K. (1996) *Plant Physiol.* **111**, 433–440.
45. Lohse, G. & Hedrich, R. (1992) *Planta* **188**, 206–214.
46. Allen, G. J., Kuchitsu, K., Chu, S. P., Murata, Y. & Schroeder, J. I. (1999) *Plant Cell* **11**, 1785–1798.
47. Klusener, B., Young, J. J., Murata, Y., Allen, G. J., Mori, I. C., Hugouvieux, V. & Schroeder, J. I. (2002) *Plant Physiol.* **130**, 2152–2163.
48. Yamazaki, D., Yoshida, S., Asami, T. & Kuchitsu, K. (2003) *Plant J.* **35**, 129–139.
49. Schultz, T. F. & Quatrano, R. S. (1997) *Plant Sci.* **130**, 63–71.
50. Jeannette, E., Rona, J. P., Bardat, F., Cornel, D., Sotta, B. & Miginiac, E. (1999) *Plant J.* **18**, 13–22.
51. Ghelis, T., Dellis, O., Jeannette, E., Bardat, F., Cornel, D., Miginiac, E., Rona, J. P. & Sotta, B. (2000) *FEBS Lett.* **474**, 43–47.
52. Li, J., Wang, X. Q., Watson, M. B. & Assmann, S. M. (2000) *Science* **287**, 300–303.
53. Bertauche, N., Leung, J. & Giraudat, J. (1996) *Eur. J. Biochem.* **241**, 193–200.
54. Leung, J., Merlot, S. & Giraudat, J. (1997) *Plant Cell* **9**, 759–771.